ELSEVIER

International Journal of Mass Spectrometry 219 (2002) 457–473

International Journal of Mass Spectrometry

www.elsevier.com/locate/ijms

Towards the characterization of the mechanism of the sequential activation of four methane molecules by Ta^+

Aude Simon, Luke MacAleese, Pierre Boissel, Philippe Maître*

Laboratoire de Chimie Physique (UMR 8000-CNRS), Université de Paris XI-Batiment 350, 91405 Orsay Cedex, France

Received 11 January 2002; accepted 19 April 2002

Dedicated to Yannick Hopilliard on the occasion of her sixtieth birthday, in recognition of her contribution to mass spectrometry, and her friendship.

Abstract

Mass spectrometry and quantum chemistry have been used to characterize the mechanism of the sequential dehydrogenation of four methane molecules by third row transition metal cation Ta^+. A comprehensive study of the second reactive intermediate $TaC_2H_4^+$ of this sequence is presented here. Mass-selected $TaC_2H_4^+$ ions have been characterized by UV–visible photodissociation showing a sequential loss of H_2 and C_2H_2. The appearance threshold of $TaC_2H_2^+$ is much higher than the corresponding thermodynamic threshold. We show that this difference is probably due to a lack of low-energy electronically excited state for the $TaC_2H_4^+$ ions formed by dehydrogenation of two methane molecules. Within the nine low-energy isomers characterized at the density functional level, the dihydridometallacyclopropene ($Ta(H)_2(C_2H_2)^+$) is the most stable. The very selective reactivity of $TaC_2H_4^+$ with both D_2 and CD_4 strongly suggests that the $Ta(H)_2(C_2H_2)^+$ is the reactive species of the sequential dehydrogenation of four methane molecules, and that the two methane dehydrogenations proceed through two successive σ-bond metatheses involving Ta^+–H and C–H σ-bonds. On the contrary, when $TaC_2H_4^+$ ions are formed by dehydrogenation of ethane, reactions with D_2 and CD_4 are less selective. The photodissociation behaviors of the corresponding ions are also very different, and the appearance thresholds of $TaC_2H_2^+$ and Ta^+ are in agreement with the corresponding thermodynamic thresholds determined theoretically. (Int J Mass Spectrom 219 (2002) 457–473)

Keywords: Gas phase reaction; Methane activation; Transition metal ion; Electronic excited states; Photo dissociation; Mass spectrometry

1. Introduction

Mass spectrometry study of the intrinsic chemical and physical properties of atomic transition metal ions interacting with selected molecules has been shown to provide interesting models for biological and catalytic processes [1]. The study of metal complexes of relevant biological molecules provides a means for understanding the structural changes induced by the coordination of the metal on a biomolecule. For example, studies of metal complexes of amino acids [2–6] allow for an understanding of the most stable form of these systems. Metal ion complexes also constitute interesting models for the understanding of transition metal-mediated activation of alkanes [7]. With this respect, it has been shown that these highly electronically and coordinatively unsaturated species are not only inherently interesting, but systematic investigations within a series of transition metals allow for a good understanding of the key steps and potential

* Corresponding author. E-mail: maitre@lcp.u-psud.fr

1387-3806/02/$ – see front matter
PII S1387-3806(02)00700-5

intermediates of the reactions between a molecule and a metal ion [8]. It is nowadays recognized that the interplay of quantum chemistry and mass spectrometry is essential for the understanding of this gas phase chemistry [7]. With this respect, it has been shown that the density functional approach, and particularly the B3LYP form, allows for a good description of these open-shell systems containing transition metal cations [9–11].

Since the first evidence that hydrocarbons may be activated by M^+ [12], numerous studies have been directed at understanding the electronic requirements for the activation of alkanes [13]. While first- and second row metal cations, with the exception of Zr^+, do not spontaneously react with methane, Irikura and Beauchamp first showed that third row metal cations are particularly reactive. In most cases, a sequential dehydrogenation of several methane molecules occurs [14] as in the case of Ta^+ where the final product is $TaC_4H_8^+$ oligomer [15].

The determination of the detailed mechanism associated with this sequential methane activation remains a challenge. In this context, a joint experimental and theoretical project is under progress in our group in order to provide more insights into the structures and energetics of the successive intermediates (i.e., MCH_2^+, $MC_2H_4^+$, $MC_3H_6^+$, and $MC_4H_8^+$) that can be observed during the sequential dehydrogenation of four methane molecules by third row transition metal cations Ta^+ and W^+. Experimentally, reactions are investigated in a Fourier transform ion cyclotron resonance (FT-ICR) mass spectrometer. Reactions with selected molecules and UV–visible photodissociation are used to characterize the mass-selected reactive intermediates. In this paper, we will show that experimental results combined with quantum chemistry provide a good understanding of the reaction mechanism of the sequential dehydrogenation of four methane molecules by Ta^+.

2. Experimental apparatus

The experimental setup has been previously described [16]. It features a FT-ICR mass spectrometer with wide optical access to the center of the trap. The trap and its surrounding are maintained to a low temperature (15–30 K) by means of a closed-cycle helium cooler insuring efficient cryopumping. Metal ions are produced by laser ablation of a Ta foil 0.1 mm thick (Goodfellow, 99.9% purity) inside the ion trap. Gases are admitted through pulsed valves. Apart from the period of neutral reactant injection, the pressure in the ion trap remains lower than 10^{-9} mbar. This, together with the mass resolution, is one of the great advantages of the experimental apparatus: spectra are not contaminated by metal oxides which are the products of very exothermic reactions. Irradiation of the ions is performed with a 75 W Xenon arc lamp focused with a silica lens. Photodissociation thresholds are determined following the technique already used [17,18] using a set of long wavelength pass colored filters with various cut-off wavelengths (305, 370, 405, 420, 435, 460, 490, 510, 525, 542, 573, 590, 624, 692, 715, 780 and 850 nm). All those filters present very similar transmission curve shapes. The mentioned wavelengths correspond to 50% transmission and, typically, 10% transmission remains 10 nm below the indicated cut-off wavelength.

3. Theoretical methods

In all calculations, the 60 inner-core electrons of Ta are described by a relativistic effective core potential [19]. The outer-core 5sp and valence electrons of Ta are described by an optimized [6s5p3d1f] contraction of a (8s7p6d1f) Gaussian basis set as proposed by Sandig and Koch on their work on the activation of a methane molecule by Ta^+ [20]. C and H atoms are represented by the polarized full double-ζ set of Dunning and Hay [21]. We have used the B3LYP [22], a hybrid density functional, as implemented in Gaussian98 [23]. The geometries and the harmonic frequencies have been determined at this level. The relative energies presented here include the zero-point vibrational energy. This method has been shown to be reliable to determine the energetics of transition metal containing systems [9–11]. Using a similar basis set for the

B3LYP approach, our calculations on reactions of W^+ with methane suggest that this approach should be accurate in the present case [18]. Two methods have been used to evaluate the vertical electronic excitations for selected systems using the basis set described previously: the configuration interaction within the singles (CIS) [24] and a time dependent density functional theory (TD-DFT) [25] method using the B3LYP density functional. The Gaussian98 program package [23] has been used throughout.

4. Experimental results

The mass spectrum recorded after reaction of pulsed methane with Ta^+ is shown in Fig. 1 the $TaC_nH_{2n}{}^+$ ($n = 0$–4) ions are formed through a sequence of dehydrogenation of four methane molecules. The pressure and the duration of the pulse are optimized so as to maximize the intensity of $TaC_2H_4{}^+$ ($m/z = 209$). After mass selection of the $TaC_2H_4{}^+$ ions, they are irradiated for 10 s with the Xenon lamp. The mass spectrum given in Fig. 2 shows the fragmentation products detected 300 ms after the end of the irradiation. The major products are by far $TaC_2H_2{}^+$ ($m/z = 207$) and Ta^+ ($m/z = 181$). The continuous ejection of $TaC_2H_2{}^+$ during the whole irradiation time indicates that a sequential fragmentation process occurs with no competition with a direct loss of C_2H_4. Other photofragments are observed, TaC_2H^+ ($m/z = 206$) and $TaC_2{}^+$ ($m/z = 205$), but since their corresponding intensities are very small and vanish with the use of filters, we will not consider these ions further.

We have determined the experimental dissociation thresholds using the method described previously. Thresholds associated with each step of the sequential loss of H_2 and C_2H_2 from $TaC_2H_2{}^+$ have been investigated. When the neutral reactant is ethane, loss of H_2 occurs even using the 850 nm long wavelength pass colored filter. That is, the appearance threshold of $TaC_2H_2{}^+$ is lower than 1.46 eV. Then, using the successive filters, the photodissociation threshold for the loss of C_2H_2 has been determined to be 2.43 ± 0.14 eV. Those results strongly contrast with the one obtained using methane in which the loss of H_2 requires more energetic photons: the experimental threshold has been determined at 2.43 ± 0.14 eV, i.e., 56.0 ± 3.0 kcal mol^{-1}. Furthermore, even after long irradiation times, the fragmentation process remains inefficient since only 11% of the parent ion is fragmented when the neutral reactant is methane (Fig. 3),

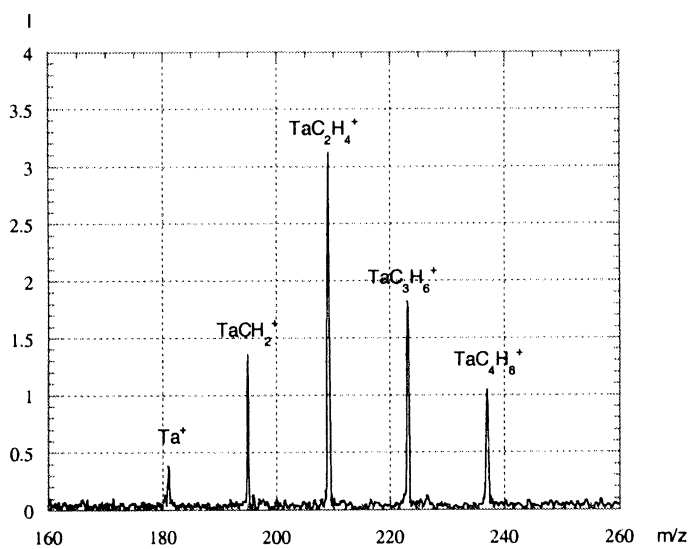

Fig. 1. Mass spectrum recorded after reaction of pulsed methane (1.5 mbars, 400 ms) with Ta^+.

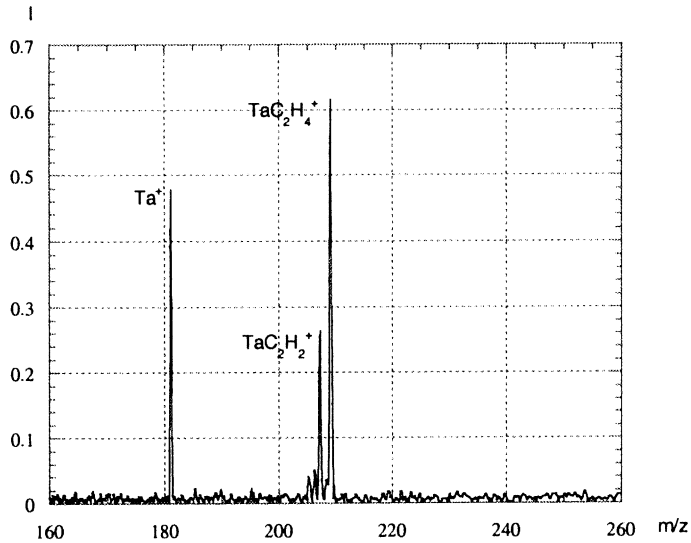

Fig. 2. Mass spectrum recorded 300 ms after irradiation without filter for 10 s of the mass-selected $TaC_2H_4^+$ ions.

whereas 84% of the $TaC_2H_4^+$ complex is fragmented when it is formed from ethane using the same filter (510 nm) (Fig. 4). That is, it was very difficult to accurately determine the threshold appearance of the Ta^+ ions in this case.

Those results strongly suggest that the $TaC_2H_4^+$ ion structures are different whether the complexes are obtained from methane or ethane. In order to go further in the insight of the probable structures of $TaC_2H_4^+$ isomers which are formed in the ICR cell,

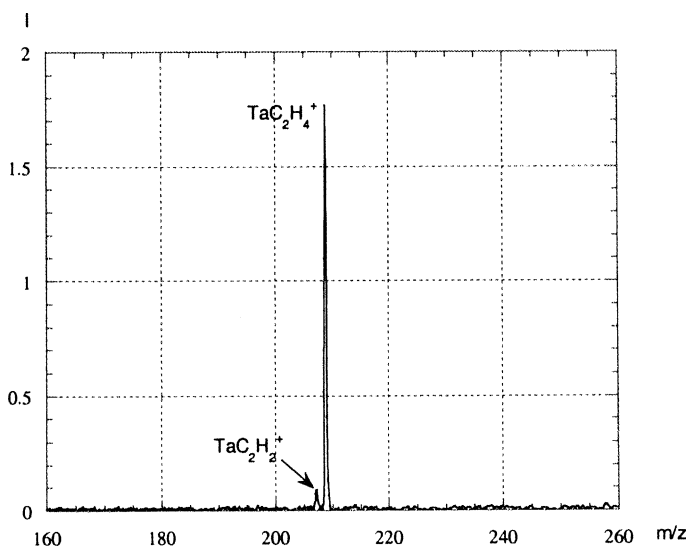

Fig. 3. Mass spectrum after photodissociation of the mass-selected $TaC_2H_4^+$ ions formed by reacting Ta^+ with methane. Ions were irradiated for 6 s through the 510 nm long wavelength pass colored filter.

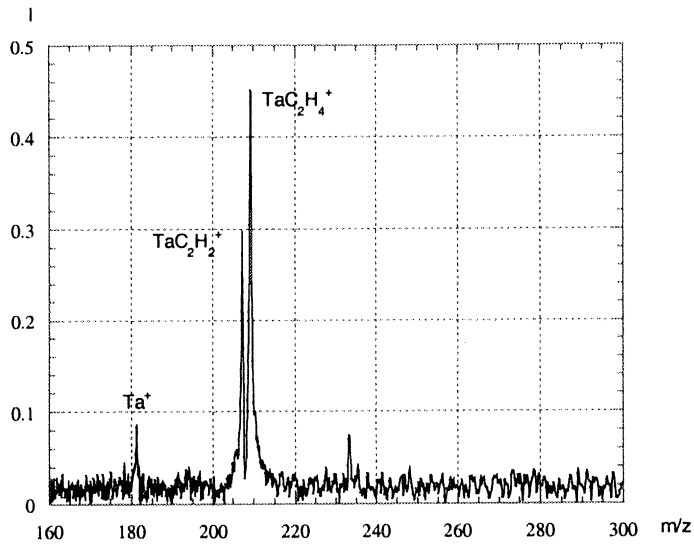

Fig. 4. Mass spectrum after photodissociation of the mass-selected $TaC_2H_4^+$ ions formed by reacting Ta^+ with ethane. Ions were irradiated for 10 s through the 510 nm long-wavelength pass colored filter.

H/D exchanges have been investigated. While the cryopumping technique allows an efficient condensation of methane on the walls of the cell, a residual pressure remains when the introduced gas is D_2. H/D exchange reactions between mass-selected $TaC_2H_4^+$ ions and D_2 have been studied using this residual pressure of D_2 (a 100 ms pulse under 1 mbar has been used). The spectra observed after the first detection, 2.5 ms after the $TaC_2H_4^+$ complex selection, are represented in Fig. 5 (methane) and Fig. 6 (ethane). One can see that

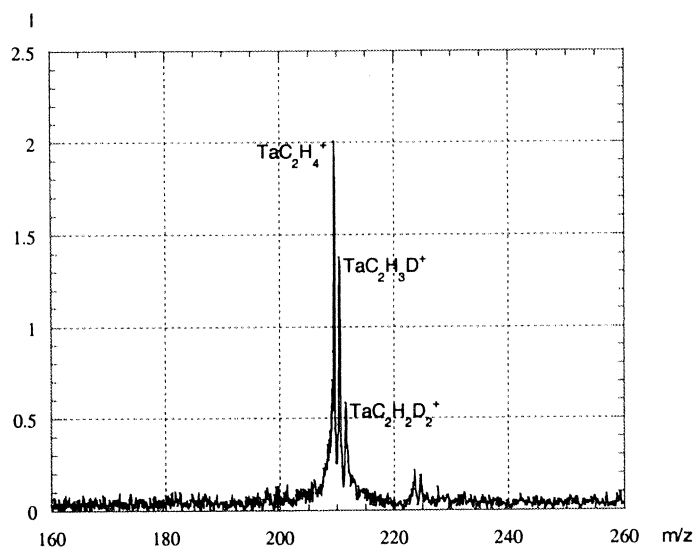

Fig. 5. Mass spectrum recorded 2.5 s after mass-selection of the $TaC_2H_4^+$ ions formed by reacting Ta^+ with methane in a residual pressure of D_2.

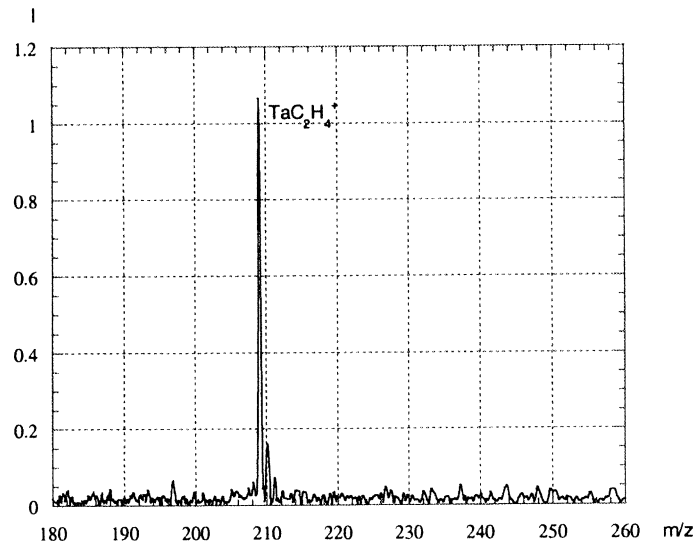

Fig. 6. Mass spectrum recorded 2.5 s after mass-selection of the $TaC_2H_4^+$ ions formed by reacting Ta^+ with ethane in a residual pressure of D_2.

the H/D exchange is much more efficient when the $TaC_2H_4^+$ ions are formed from methane where 49% of the ions undergo one or two H/D exchanges. Only 17% of the parent ion formed from ethane is deuterated and the exchange reactions remain inefficient even when a pulse of D_2 is introduced in the ion trap after the mass selection of $TaC_2H_4^+$. We will come back to the kinetics of the H/D exchange in Section 6.

Other evidences for the influence of the formation pathways on the structure of $TaC_2H_4^+$ are

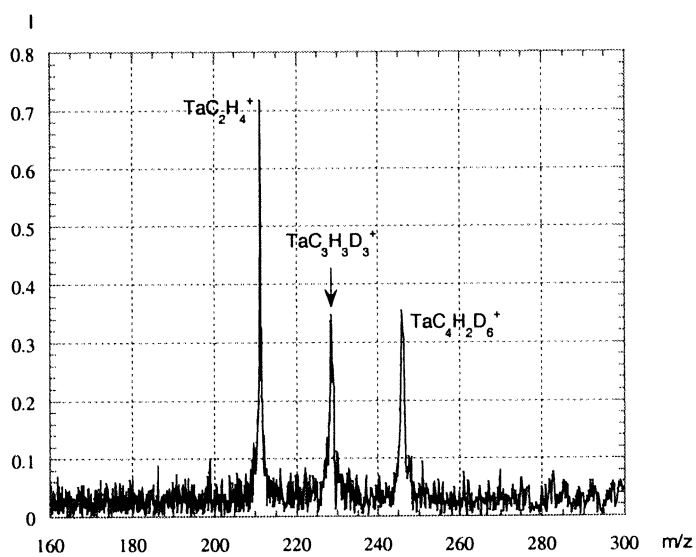

Fig. 7. Mass spectrum recorded after 300 ms reaction between CD_4 and mass-selected $TaC_2H_4^+$ ions formed by reacting Ta^+ with methane.

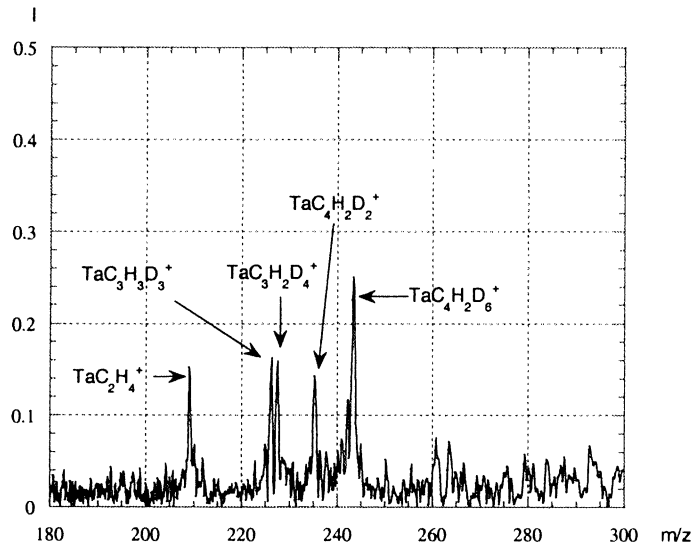

Fig. 8. Mass spectrum recorded after 300 ms reaction between CD_4 and mass-selected $TaC_2H_4^+$ ions formed by reacting Ta^+ with ethane.

also given by the reactions of this ion with CD_4. After the mass selection of $TaC_2H_4^+$ formed by $Ta^+ + 2CH_4$, a 400 ms pulse of CD_4 at 2 mbars has been injected into the reaction cell. The spectrum recorded 300 ms after the end of the pulse (Fig. 7) shows that two successive reactions occur and the major primary product is $TaC_3H_3D_3^+$ ($m/z = 226$) whereas the major secondary product is $TaC_4H_2D_6^+$ ($m/z = 243$). This spectrum shows that the two successive reactions are very selective, each one corresponding to an addition of CD_4 followed by an elimination of HD. There is nearly no scrambling: minor product such as $TaC_3H_2D_4^+$ ($m/z = 227$) appears with a very small intensity. When $TaC_2H_4^+$ formed from ethane reacts with CD_4, the spectrum (Fig. 8) obtained in the same experimental conditions is very different. Nearly the same amount of $TaC_3H_3D_3^+$ ($m/z = 226$) and $TaC_3H_2D_4^+$ ($m/z = 227$) is produced and two secondary products are also formed: $TaC_4H_2D_6^+$ ($m/z = 243$) as in the case of methane and $TaC_4H_2D_2^+$ ($m/z = 235$). The $TaC_2H_4^+$ ions produced from ethane react less specifically with CD_4 than the ones produced from methane.

5. Relative energies of the $TaC_2H_4^+$ isomers: theoretical results

Electronic structure calculations have been performed in order to rationalise the experimental results. The extensive study of the mechanisms of the reactions of Ta^+ with methane and ethane is under completion, but some relevant elements will be given in Section 6. In this paper, we essentially focus on the characterization of the lowest lying isomers of $TaC_2H_4^+$. Nine isomers have been found to be thermodynamically stable with respect to the $Ta^+ + C_2H_6$ asymptote and their geometries are given in Fig. 9. The energies of these isomers are reported in Table 1. As can be seen, only three isomers are found to be thermodynamically stable with respect to the $Ta^+ + 2CH_4 - H_2$ asymptote. Therefore, as expected, the reaction with methane is more selective than the reaction with ethane on a pure thermodynamical ground.

In their pioneering work on the sequential reactions of methane with third row transition metal cations, Irikura and Beauchamp [14] suggested possible structures for the $MC_nH_{2n}^+$ ions, and in the case of $MC_2H_4^+$, an M^+–olefin structure was proposed.

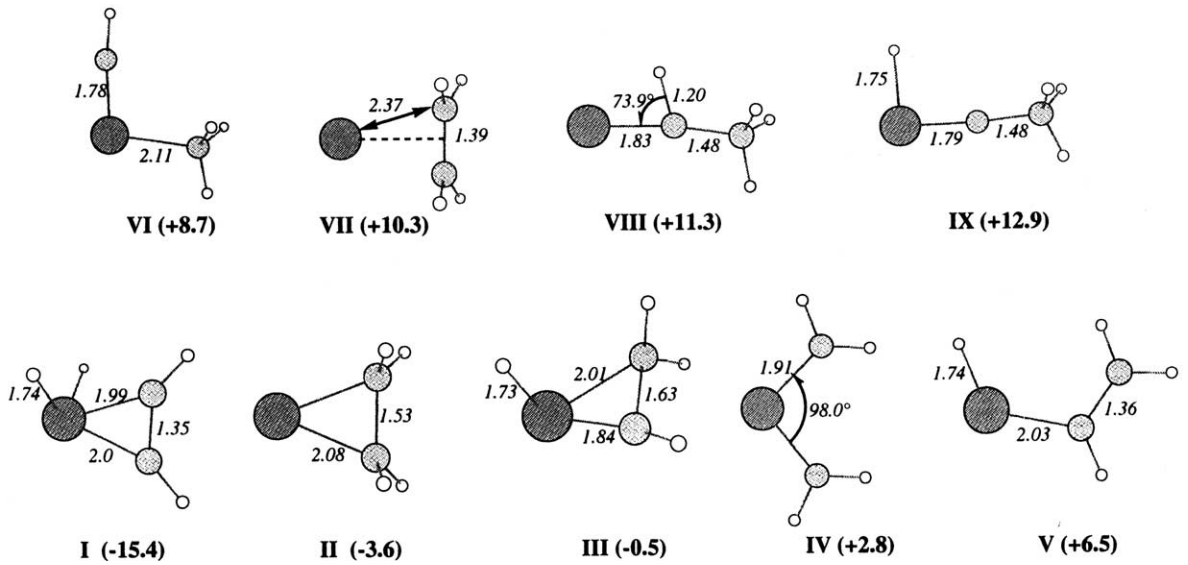

Fig. 9. Optimized parameters of the nine lowest isomers of $TaC_2H_4^+$ characterized at the B3LYP level. Bond lengths are in Å and angles in degrees (°).

We found that this isomer (**VII**) could be formed by the dehydrogenation of C_2H_6 by Ta^+, but not from the successive dehydrogenations of two methane molecules. Six other isomers are more stable than the M^+–olefin complex. The most stable isomer (**I**) presents two hydrides and one metallacyclopropene unit. Interestingly, we found that this metallacyclopropene unit is also present in the lowest energy isomer of $MC_3H_6^+$ and $MC_4H_8^+$ for both M = Ta and M = W, each hydride being substituted by one and two methyl groups, respectively.

Three types of spin states are thus expected depending on the number of covalent bonds formed with Ta^+. Structures of each type have been found and can be presented starting from the metal–olefin complex. The ground electronic state of this Ta^+ ethylenic complex (**VII**), with no covalent metal–ligand bond, is the only structure presenting a ground state ($^5A_2$) with a quintet

Table 1
Most stable $TaC_2H_4^+$ isomers

Name	Symmetry state	Figure label	Relative energies	Lowest allowed electronic transition *CIS*-TD-DFT	$TaC_2H_4^+ \rightarrow TaC_2H_2^+ + H_2$ thermodynamic threshold
$HHTaC_2H_2^+$	^1A	**I**	−15.4	*89.5*-75.6 (^1A)	26.9
$TaC_2H_4^+$	$^3A_2$	**II**	−3.6	*11.3*-9.3 ($^3B_1$)	15.2
$HTa(CHCH_2)^+$	^1A	**III**	−0.5	*49.7*-45.6 (^1A)	12.0
$Ta(CH_2)_2^+$	$^1A_1$	**IV**	2.8	*44.9*-37.6 ($^1B_1$)	8.7
$HTaC_2H_3^+$	^3A	**V**	6.5	*11.6*-10.7 (^3A)	5.0
$(CH_3)TaCH_4^+$	$^1A'$	**VI**	8.7	*34.7*-20.4 (^1A)	2.8
$TaC_2H_4^+$	$^5A_2$	**VII**	10.3	*10.3*-6.3 ($^5B_1$)	1.2
$Ta(CHCH_3)^+$	$^1A'$	**VIIII**	11.3	*20.8*-17.8 (^1A)	0.2
$HTa(CCH_3)^+$	$^1A'$	**IX**	12.9	*29.4*-18.0 (^1A)	−1.4

In column 3, labels of Fig. 9 are given. In column 4, relative energies are given relative to the $Ta^+ + 2CH_4 - 2H_2$ asymptote (absolute energy of isomer **I** is −135.28115319 a.u. at the B3LYP/1 level). In column 5, vertical excitation energies corresponding to the lowest allowed electronic transition are given at the CIS (in italic) and TD-B3LYP levels. All reported energies are in kcal mol^{-1}.

spin state, as the ground state of $Ta^{+5}F(s^1d^3)$ [26]. The corresponding optimized structure (Fig. 9) shows that the CC double character is essentially retained with a CC distance of 1.39 Å. One alternative is to form two Ta^+–C covalent bonds and this leads to a metallacyclopropane structure (**II**) in a triplet state ($^3A_2$) with an optimized structure presenting a typical single bond CC (1.53 Å). As can be seen in Table 1, the inserted species is more stable than the ion–molecule complex by 13.9 kcal mol^{-1}. This shows the capability of third row transition metal cations to form strong covalent bonds [27]. One can also consider that Ta^+ inserts into a CH bond of C_2H_4 and forms a Ta^+–C and a Ta^+–H covalent bond. This leads to a hydridovinyl complex (**V**) in a triplet state (^3A) lying 21.9 kcal mol^{-1} above the lowest energy isomer and thus less stable than the metallacyclopropane. From the hydridovinyl complex (**V**), Ta^+ can insert into the π-CC bond of the vinyl unit leading to a metallacycle (**III**) with a Ta^+C double bond (1.84 Å), a Ta^+C single bond (2.01 Å) and a Ta^+–H bond (1.73 Å). The corresponding ground state is thus a singlet spin state. As can be seen in Table 1, the insertion into the π-CC bond of the vinyl unit is favorable (**III** is 7 kcal mol^{-1} lower in energy than **V**) and the resulting isomer (**III**) lies only 14.9 kcal mol^{-1} above the lowest energy structure. From structure **III**, the lowest energy structure (**I**) is formally obtained by an insertion of Ta^+ into a CH bond of the CH_2 group. The optimized structure of the metallacyclopropene unit displays a characteristic CC bond length (1.35 Å).

Structures **VIII** and **IX** derive from the interaction of Ta^+ with the methylcarbene, 66.3 kcal mol^{-1} higher in energy than the ethylene isomer at the present level of calculation, and they have been found respectively 26.7 and 28.3 kcal mol^{-1} above **I**. The optimized structure of the carbene complex (**VIII**) presents a strong agostic deformation, characterized by a substantial lengthening of a CH bond (1.20 Å). Agostic interactions are characteristic of unsaturated organometallic systems, but seem to be more pronounced in the case of third row transition metal cations than with their first- or second row analogues [18]. The insertion into this CH bond leads to a hydridomethylmethylidine complex (**IX**) characterized by a short Ta–C triple covalent bond (1.79 Å) and a Ta–H bond (1.75 Å).

The two structures left (**IV** and **VI**) formally correspond to the insertion of Ta^+ into the CC bond of the two C_2H_4 isomers. Insertion into the double bond of ethylene leads to the biscarbene structure (**IV**) with two double covalent Ta^+C bonds and the electronic ground state is a singlet. The corresponding optimized structure (**IV**) lies 18.2 kcal mol^{-1} above **I**. Insertion into the CC bond of the methylcarbene isomer leads to Ta^+ triply bound to a CH unit (1.78 Å) and a methyl group (2.11 Å) and the corresponding singlet ground state is 24.1 kcal mol^{-1} higher than structure **I**.

The reaction of Ta^+ with ethane could lead to the nine isomers, the exothermicity of the reaction ranging from −33.1 kcal mol^{-1} for isomer **I** to −4.9 kcal mol^{-1} for isomer **IX**. In the case of the reaction with methane, only the three isomers the lowest in energy could be obtained (Table 1): the formation of isomer **I** is exothermic by −15.4 kcal mol^{-1} and the one of isomers **II** and **III** by −3.6 and −0.5 kcal mol^{-1}, respectively.

6. Discussion

The experimental data give several evidences that the $TaC_2H_4^+$ ions produced by the dehydrogenation of ethane are different from the ones produced by a sequential dehydrogenation of two methane molecules. Electronic structure calculations confirm that, from a thermodynamic point of view, the situation is complicated since at least nine isomers of $TaC_2H_4^+$ could be formed in the former case and three in the latter. Nevertheless, the high selectivity of the reactions of $TaC_2H_4^+$ produced from methane with deuterated dihydrogen and methane strongly suggests that the $(H)_2TaC_2H_2^+$ isomer **I**, predicted as the lowest-lying isomer by theory, plays an important role in these reactions. Indeed, this isomer presents two Ta^+–H bonds, and therefore the successive reactions with D_2 or CD_4 could be the result of sequences of two σ-bond metathesis (Scheme 1), reactions which are known

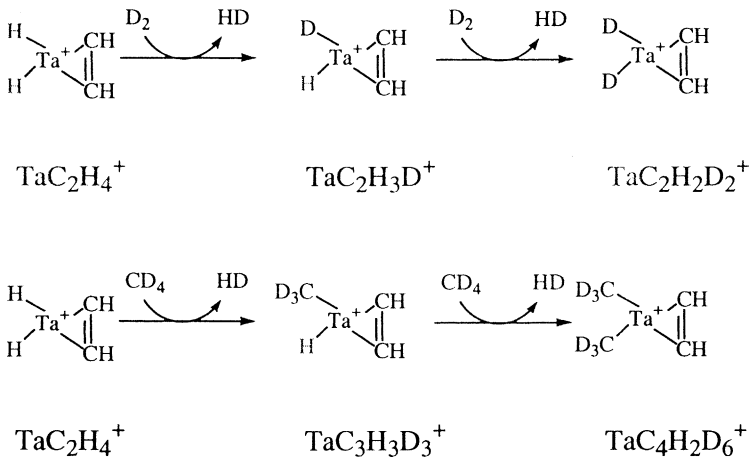

Scheme 1.

to proceed through low-energy four centers transition states [28].

Furthermore, this interpretation would also be consistent with both theoretical and experimental results. First, $(H)(Me)TaC_2H_2^+$ and $(Me)_2TaC_2H_2^+$ are predicted as being the most stable isomers of $TaC_3H_6^+$ and $TaC_4H_8^+$, respectively. Second, the comparison of the kinetic of the H/D scrambling observed when D_2 reacts simultaneously with $TaC_2H_4^+$, $TaC_3H_6^+$ and $TaC_2H_8^+$ shows that no H/D scrambling occurs in $TaC_4H_8^+$, while $TaC_3H_6^+$ exchanges one H at the same rate as $TaC_2H_4^+$ does exchange one or two H. One could then conclude that the reactive ions corresponding to $TaC_2H_4^+$ and $TaC_3H_6^+$ involved in the activation of methane are $(H)_2TaC_2H_2^+$ and $(H)(Me)TaC_2H_2^+$, respectively.

Nevertheless, the detailed analysis of photofragmentation processes as well as of the kinetics of the H/D exchange in $TaC_2H_4^+$ suggests that the situation is probably more complicated as we will be seen in the next section.

6.1. Kinetic of the H/D exchange

While $TaC_2H_4^+$ ions formed from ethane react very slowly with D_2, the ions resulting from the dehydrogenation of two methane molecules undergo two fast H/D exchanges with D_2. The evolution of the relative intensities of the three ions $TaC_2H_4^+$, $TaC_2H_3D^+$, and $TaC_2H_2D_2^+$ is given in Fig. 10. As previously mentioned, two fast H/D exchanges could be the signature of the reaction of $(H)_2TaC_2H_2^+$ through two successive σ-bond metathesis. Nevertheless, after 15 s of reaction, the H/D exchange ends (Fig. 10) but the populations of the $TaC_2H_4^+$ and $TaC_2H_3D^+$ ions are still significant. This kinetic behaviour rather suggests that the reaction cell does not only contain the $(H)_2TaC_2H_2^+$ isomer. A reasonable assumption would be that the three $TaC_2H_4^+$ isomers (**I**, **II**, and **III**), predicted to be thermodynamically stable with respect to the $Ta^+ + 2CH_4$ by theory, coexist in the reaction cell. While one fast H/D exchange can be expected with **III** through a σ-bond metathesis as in **I**, an H/D exchange with **II** would involve more significant rearrangements. That is, the population of the $TaC_2H_4^+$ and $TaC_2H_3D^+$ ions at long reaction time would, respectively, correspond to isomers **II** and d-**III** (deuterated isomer **III**) as summarized in Scheme 2.

The results of the fit of the experimental data are given in Fig. 10. We have assumed that all the reactions are pseudo-first order with respect to the ion, the D_2 pressure being constant. Three parameters have been optimized: a pseudo-first order rate constant K common for the three H/D exchanges, and the relative initial populations of **I** and **III**. The

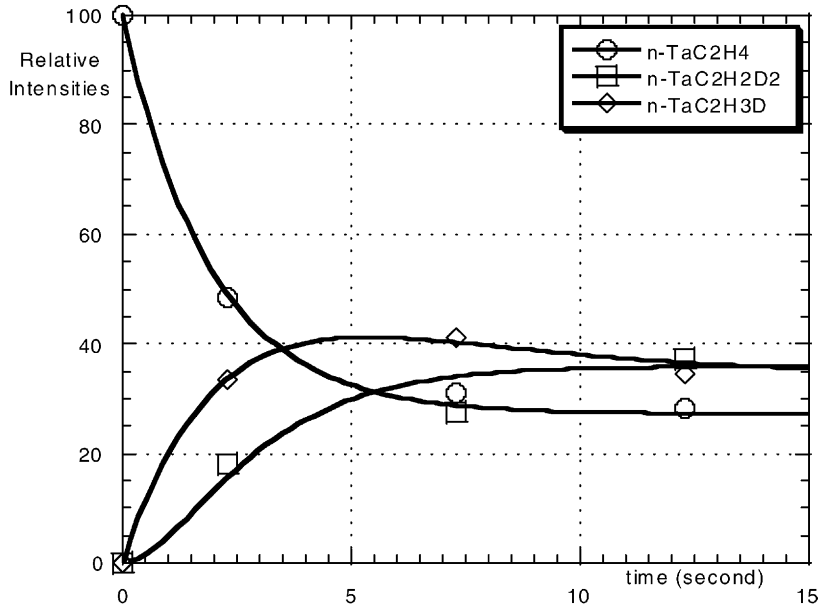

Fig. 10. Kinetics of the H/D exchange of the $TaC_2H_4^+$ ions formed from methane. Experimental relative intensities of the $TaC_2H_4^+$, $TaC_2H_3D^+$, and $TaC_2H_2D_2^+$ ions as a function of the time (scattered curves). Full lines are obtained according to the fit described in Scheme 1.

optimized values of the parameters suggest that the initial population of isomers **I** and **III** are nearly the same (ca. 36%) and the optimized value of K is $0.5\,s^{-1}$. Assuming that the temperature and pressure of the reaction are 30 K and 10^{-9} mbar, respectively, a rate constant $2 \times 10^{-9}\,cm^3$ per molecule s^{-1} can be derived. This value would be of the order of magnitude of the capture collision rate assuming an ion-induced dipole interaction with a D_2 polarisability equal to $0.72\,Å^3$. Those results suggest that the low activation energy σ-bond metathesis could be a good candidate for these fast H/D exchanges.

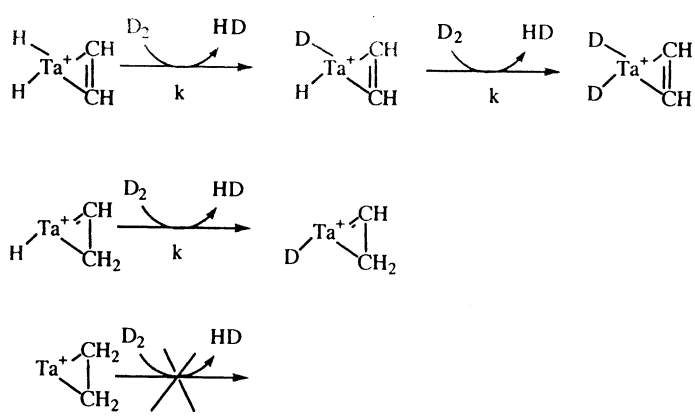

Scheme 2.

6.2. Reaction mechanisms

Kinetics factors are also expected to play an important role. The fact that the initial population of the three isomers as optimized above are nearly equal (36% of **I**, 36% of **III** and 28% of **II**) might suggest that during the reaction of $TaCH_2^+ + CH_4$, the system has to proceed through a rate limiting step common to the three reaction channels leading to the isomers **I**, **II** and **III**. The potential energy surface corresponding to the formation and dehydrogenation of $TaC_2H_4^+$ has been investigated. The complexity of such a mechanistic study is due to the fact that a reaction such as $TaCH_2^+ + CH_4$ is likely to involve quintet, triplet and singlet spin states and going from one surface to another is being possible for organometallic systems containing third row transition metals through strong spin–orbit coupling [29,30].

The reaction mechanism leading to the formation of $TaC_2H_4^+$ isomers **I**, **II**, and **III** is depicted in Fig. 11 where we give the relative energies of the intermediates relative to the $Ta^+ + 2CH_4 - H_2$ asymptote. The geometrical structure of the transition states of interest are given in Fig. 12. We found that the lowest energy path leading to the CH_4 activation is not the direct insertion of Ta^+ into a CH bond. Instead, we found that the activation proceeds through the addition of a methane C–H bond to a π bond of the metal-methylidine to form the $(CH_3)(H)Ta(CH_2)^+$ (**2**), the most stable intermediate among all those which were calculated.

Furthermore, this step is not the rate limiting step: the transition state $\mathbf{TS_{1-2}}$ connecting (**2**) and the

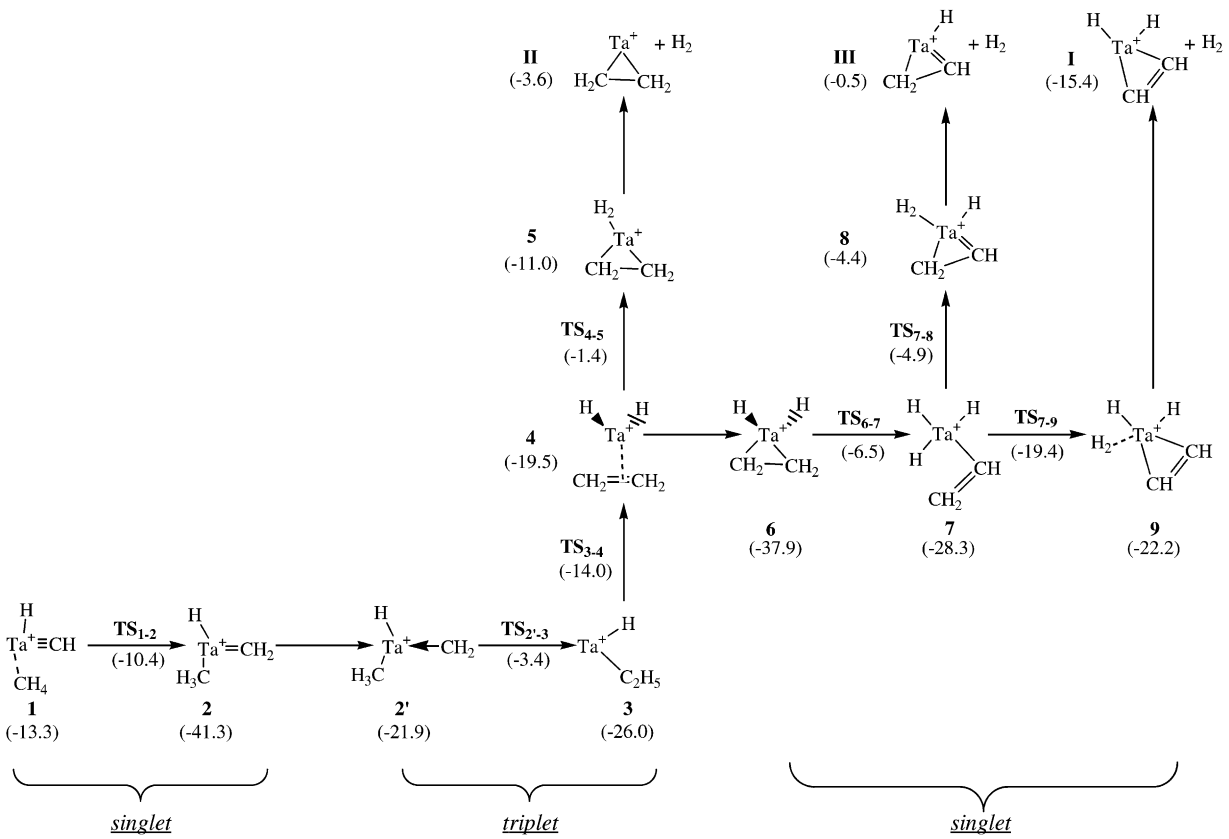

Fig. 11. Reaction mechanism associated to the dehydrogenation of the second molecule of methane by Ta^+. Energies in kcal mol^{-1} are relative to the $Ta^+ + 2CH_4 - H_2$ asymptote.

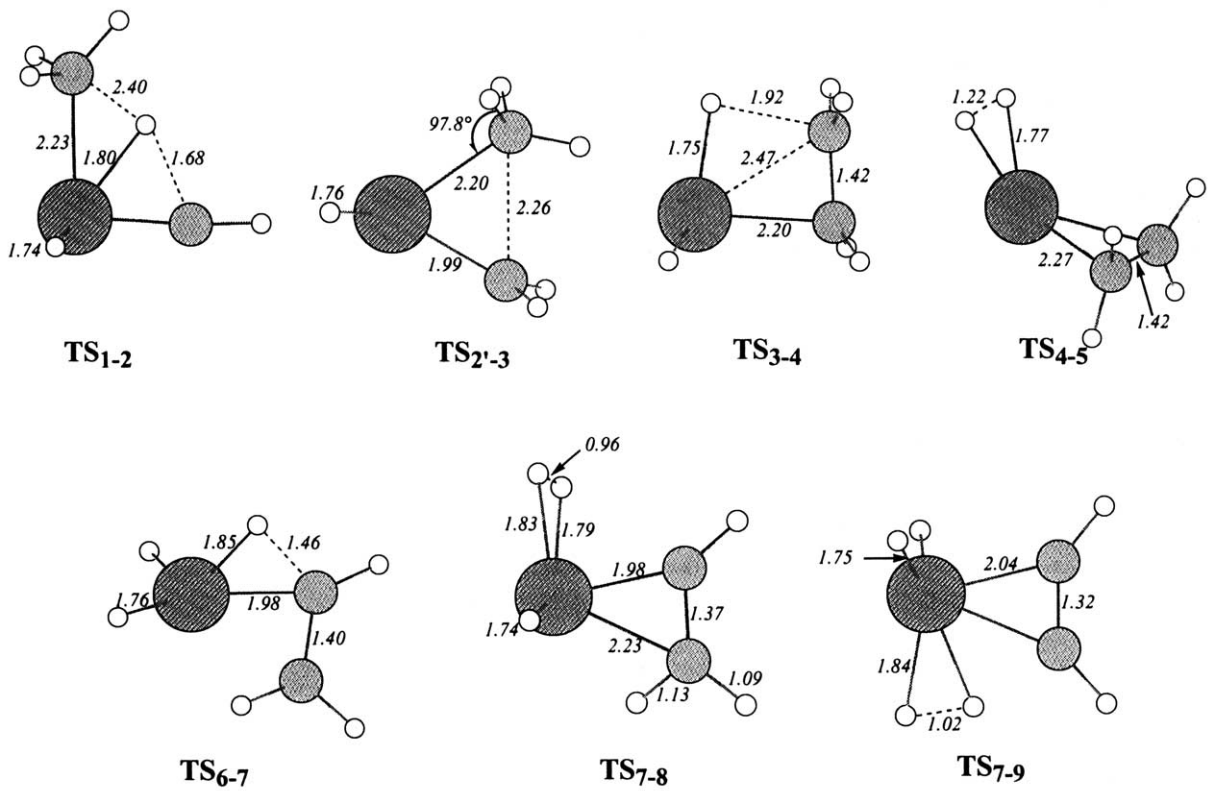

Fig. 12. Structure of the transition states associated to the mechanism depicted in Fig. 11. Bond lengths are in Å and angles in degrees (°).

molecular complex of methane $(CH_4)Ta(H)(CH)^+$ (**1**), lies only 2.9 kcal mol^{-1} above (**1**), and the corresponding imaginary frequency is $-i1105\,cm^{-1}$. This is in contrast with the first dehydrogenation reaction $Ta^+ + CH_4 \rightarrow TaCH_2^+ + H_2$ theoretically studied by Sandig and Koch, where the rate limiting step is the oxidative addition of methane [20]. The triplet spin state complex $(CH_3)(H)Ta(CH_2)^+$ (**2′**) has also been characterized. It lies 19.4 kcal mol^{-1} above the singlet (**2**). The spin change is associated with a change in the coordination mode of the methylidene group. In **2**, there is a Ta^+=CH_2 double bond, characterized by a Ta^+–C distance of 1.89 Å, whereas in isomer **2′**, the methylidene group acts as a two-electron donor, and the Ta^+–C bond is lengthened (2.07 Å).

We found that the most efficient path leading to the CC coupling occurs on the triplet potential energy surface from $(CH_3)(H)Ta(CH_2)^+$ (**2′**) complex. The transition state **TS$_{2'-3}$** connecting this intermediate (**2′**) to the $HTaC_2H_5^+$ complex (**3**) has been characterized. **TS$_{2'-3}$**, associated with an imaginary frequency of $i339.0\,cm^{-1}$, lies only 3.4 kcal mol^{-1} below the reactants energy. Therefore, the step corresponding to C–C coupling is the rate limiting step for the formation of the three isomers **I**, **II** or **III** (Fig. 11). Then a hydrogen β-shift occurs through **TS$_{3-4}$** leading to the intermediate $(H)_2Ta(C_2H_4)^+$ (**4**) where an ethylene is bound to a dihydrido unit. An isomerisation of this intermediate leads to the dihydrogen complex of the metallacyclopropane $(H_2)Ta(C_2H_4)^+$ (**5**) which spontaneously looses H_2 to lead to the $TaC_2H_4^+$ metallacyclopropane isomer **II**. The transition state **TS$_{4-5}$** has been found to be very close to the reaction asymptote (−1.4 kcal mol^{-1}). This could be consistent

with the fact that the proportion of isomer **II** as found in the H/D kinetic modeling is lower than the ones of **I** and **III**.

The formation of the isomers **I** and **III** of $TaC_2H_4^+$ requires a triplet to singlet change which might occur through the isomerisation of **4** into the singlet spin-state dihydrometallacyclopropane intermediate $(H)_2Ta(C_2H_4)^+$ (**6**) which lies 37.9 kcal mol^{-1} below the reactant asymptote. Then this intermediate may lead to the trihydrovinyltantalum $(H)_3Ta(CHCH_2)$ complex (**7**) lying 28.3 kcal mol^{-1} below the asymptote via the transition state $\mathbf{TS_{6-7}}$ associated with insertion of Ta^+ into an α-CH bond. The next step leading to the formation of the isomer **III** involves a concerted reductive elimination of H_2 and a coordination change of the vinyl unit leading to the intermediate (**8**). The corresponding transition state $\mathbf{TS_{7-8}}$ is just above (**8**). An alternative channel leads to the formation of **I**. It starts with a concerted reaction. Indeed, a low-energy transition state $\mathbf{TS_{7-9}}$ has been located and it is associated with a concerted intramolecular β-migration of H and H–H reductive elimination to form the $(H_2)(H)_2Ta(C_2H_2)^+$ intermediate (**9**) which leads to isomer **I** after loss of H_2. As can be seen in Fig. 11, the rate limiting step for the formation of isomers **I** and **III** is the CC coupling.

6.3. Photofragmentation processes

The photofragmentation behaviour of the $TaC_2H_4^+$ ions strongly depends on the formation process. Although a similar $TaC_2H_4^+ \rightarrow TaC_2H_2 \rightarrow Ta^+$ sequential process occurs, the threshold appearance of $TaC_2H_2^+$ is significantly higher when the $TaC_2H_4^+$ ions are formed by the dehydrogenation of two methane molecules (2.43 ± 0.14 eV) rather than one ethane (<1.46 eV). Electronic structure calculations have been performed to compare thermodynamic and photodissociation thresholds. The $TaC_2H_2^+$ ion has been characterized as an inserted complex with two Ta^+C covalent bonds: its ground state is a triplet spin state ($^3A_2$), and the geometrical parameters of the metallacyclopropene unit (TaC = 1.983 Å, CC = 1.365 Å, CCH = 135.6°) are essentially similar to the ones in **I**. They are also similar to the ones of the lowest energy isomer ($^4A_2$) of the $WC_2H_2^+$ ion characterized by Gee et al. [17] (WC = 1.958 Å, CC = 1.350 Å, CCH = 141.00). This structure lies very low in energy. Indeed, in agreement with the experiment showing that two spontaneous dehydrogenations of ethane by Ta^+ are observed, the reaction enthalpy associated with the double dehydrogenation of ethane has been found to be −6.3 kcal mol^{-1}. The thermodynamic thresholds associated with the dehydrogenation of each the isomers of $TaC_2H_4^+$ are small and the largest value, obtained for the dehydrogenation of **I**, is 26.9 kcal mol^{-1} (or 1.17 eV) (see Table 1).

The $TaC_2H_4^+$ ions made by dehydrogenation of ethane are characterized by a small photodissociation threshold for the loss of H_2 since $TaC_2H_2^+$ ions are observed even when the 850 nm long wavelength pass color filter is used. That is, the appearance threshold of $TaC_2H_2^+$ is lower than 1.46 eV or 33 kcal mol^{-1}. When the neutral reactant is methane, on the contrary, the loss of H_2 from $TaC_2H_4^+$ is only observed with photons of 2.43 eV (56.0 kcal mol^{-1}) energy or higher, value which is much higher than all the predicted thermodynamic thresholds. Among other factors [31], one could think that the origin of the large photodissociation threshold could be due to a lack of low-energy electronic excited states for the $TaC_2H_4^+$ ions. Thus, vertical excitations to the lowest electronic excited states have been calculated for the nine $TaC_2H_4^+$ isomers and the energy corresponding to the lowest transition is given in Table 1. At both levels of theory, one can see that the electronic spectra of the different isomers are very different. While the ethylenic complex **VII** presents a low-lying excited state at only 4.1 kcal mol^{-1}, the first excited electronic state of the dihydrometallacyclopropene complex **I** is very high in energy (75.6 kcal mol^{-1}). An inspection of Table 1 reveals that in the case of triplet or quintet spin states, as in the case of isomers **II**, **V**, and **VII**, the first excited state is systematically low in energy (4.1–10.7 kcal mol^{-1}). These electronic transitions correspond to an excitation of a non-bonding d electron. In the case of singlet spin states, two cases should be distinguished. When a

weak π metal–ligand bond is involved, such as in **III**, **IV**, **VI**, **VIII**, and **IX**, there is a relatively low-lying excited state corresponding to a charge-transfer from a metal–ligand bond to an empty d orbital. On the other hand, structure **I** is unique since Ta^+ is engaged in four σ covalent bonds. This is not surprising to find the first excited electronic state very high in energy since it corresponds to the charge-transfer from a metal-hydride to an empty d orbital.

In the case of ethane, the nine isomers are thermodynamically accessible and six of them (**II**, **V**, **VI**, **VII**, **VIII**, and **IX**) present low-energy excited states which lie less than 1 eV above the ground states. Therefore, the $TaC_2H_2^+$ ions observed when the 850 nm long wavelength pass colored filter could be produced from these isomers. Interestingly, by monitoring the percentage of the photodissociated $TaC_2H_4^+$ ions as a function of the filter cut-off wavelengths, one can observe that at 510 nm the percentage of photo-dissociated ions increase from 35 to 50% suggesting that electronic excited states of other isomers can be reached. In the case of methane, the high energy photodissociation threshold 2.43 eV (56.0 kcal mol^{-1}) obtained could be the signature of the exclusive formation of isomers presenting electronically excited states only at high energy. With this respect, the isomers **I** and **III**, which are predicted by theory to be accessible kinetically and thermodynamically, could be the good candidates (see Table 1). Nevertheless, one could not also exclude the isomer **IV** since its formation is predicted to be only slightly endothermic (+2.8 kcal mol^{-1}). The fact that the thermodynamic threshold for the loss of H_2 from **I** is predicted to be larger than the observed photodissociation thresholds of the ions produced from methane does not exclude this isomer. Indeed, the formation of isomer **I** is predicted to be very exothermic (−15.4 kcal mol^{-1}) and one cannot exclude an incomplete cooling of this isomer which could shift the photodissociation threshold to lower energy. Furthermore, the prediction of the relative energies of the excited states of the present ions constitutes a difficult task and the TD-B3LYP might overestimate the electronic excitation energy.

7. Conclusions and perspectives

The characterization of the reaction intermediates associated with the activation of alkanes is quite complex. This work confirms that the combination of experiments and electronic structure calculations helps towards this end. The integration of spin–orbit coupling in the exploration of the potential energy surface would singularly improve the characterization of the present system. Nevertheless, considering its dimensionality, an extensive exploration would remain difficult. This work shows that when Ta^+ reacts with methane, the mass-selected $TaC_2H_4^+$ ions, formed after the consecutive dehydrogenation of two methane molecules, react very specifically with D_2 and CD_4. Reactions with CD_4 suggest that the reactive $TaC_2H_4^+$ ions are probably the ones presenting the $(H)_2TaC_2H_2^+$ structure **I**, found to be the lowest energy structure by theory. This would be also consistent with the high energy photodissociation thresholds associated with the loss of H_2. Nevertheless, the analysis of the kinetic of the H/D exchange reactions between D_2 and $TaC_2H_4^+$ ions reveals that three isomers probably coexist in the reaction cell.

Infrared would offer an alternative method for the structural characterization of the ions M^+. Due to the low density of the ions in the ICR cell, infrared absorption techniques are impossible. Yet, IR spectrum can be derived by monitoring the fragments formed through an infrared photoinduced dissociation after exciting a vibrational transition of the parent ion M^+. Such IR spectroscopy of M^+ in the gas phase has been achieved by using the so-called "messenger" technique where a weakly bound complex ion $(M-m)^+$ is made between the ion of interest M^+ and the messenger m, which is typically a rare gas [32,33]. The weak interaction between M^+ and m not also insures a weak perturbation of the vibrational signature of M^+ but also that the dissociation threshold $M^+ + m$ would be reached after absorption of one infrared photon by the complex ion $(M-m)^+$. More recently, several studies have shown that the use of an intense and tuneable IR source such as the one provided by a free-electron laser allows for the derivation of

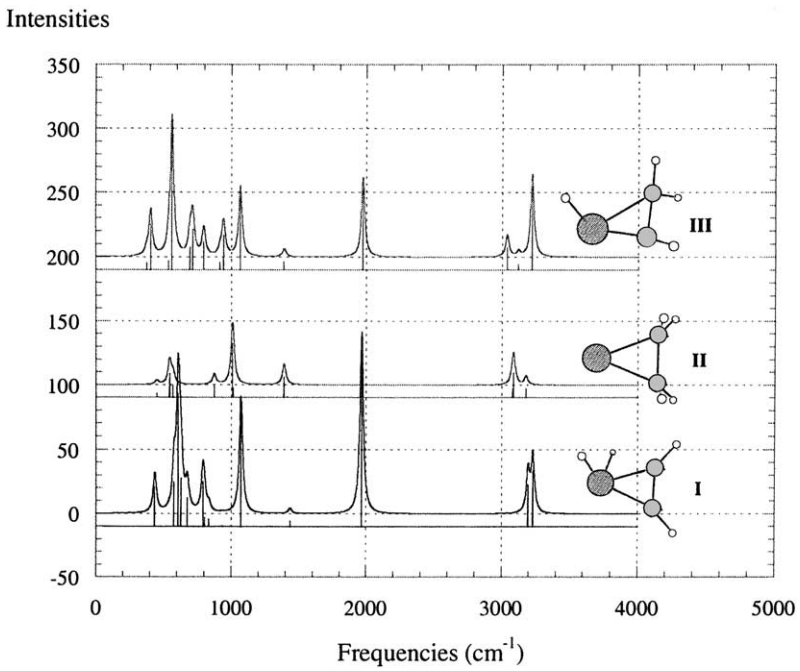

Fig. 13. Calculated infrared spectrum of the three lowest-energy isomers (**I**, **II**, and **III**) of $TaC_2H_4^+$. The discrete spectra determined at the B3LYP level have been convoluted with a 30 cm^{-1} FWHM Lorentzian line profile.

the IR spectrum of polyatomic ions isolated in an ion trap [34,35]. Resonance-enhanced multiphoton dissociation (IR-REMPD) is achieved and the IR spectrum is obtained by monitoring the intensity of the fragment ion as a function of the wavelength. The efficiency of such a multiphoton process strongly relies on the IVR which has to take place in order to allow for a resonant absorption in the same vibrational mode [36]. The comparison of the density of vibrational states of the $TaC_2H_4^+$ ion, determined for several isomers of interest, to the one of PAH [34] which have been characterized by IR-REMPD, suggests that the efficiency of the IVR process should be sufficient to induce dissociation in the present case.

The vibrational spectra of the nine isomers of $TaC_2H_4^+$ have been characterized and the spectra of the representative isomers (**I**, **II**, and **III**) are given in Fig. 13. As can be seen in Fig. 13, within the 1600–2000 cm^{-1}, only one band appears. The analysis of the normal modes reveals that it corresponds to the Ta^+–H stretching which ranges between 1925 and 1973 cm^{-1} according to the isomers **I** and **III**. That is, a dissociation of $TaC_2H_4^+$ into $H_2 + TaC_2H_2^+$ induced by an irradiation at this wavelength would demonstrate the presence of an isomer presenting a metal-hydride bond. The only isomer showing a band above 2000 cm^{-1} is the one which presents an ethylidene ligand (isomer **VIII**), the peak at 2252 cm^{-1} corresponding to the C–H stretching of the terminal methyl group. The distinction between the different isomers also appears in the bending frequencies prior to 1200 cm^{-1}. For example, the biscarbene complex (isomer **IV**) presents no signal between 500 and 1200 cm^{-1} except a very intense peak at 788 cm^{-1} that can be attributed to the out of plane bending of the methylidene group. Therefore, we plan to conduct IR direct characterization experiments coupling the mobile FT-ICR MICRA (mobile ion cyclotron resonance apparatus) which is under development in

our laboratory to the infrared radiation emitted by the free-electron laser CLIO [37] at LURE.

Acknowledgements

The authors would like to thank R. Thissen, J. Lemaire and P. Pernot for fruitful discussions.

References

[1] B.S. Freiser, Organometallic Ion Chemistry, Kluwer Academic Publisher, Dordrecht, 1996.
[2] T. Wyttenbach, M. Witt, M.T. Bowers, J. Am. Chem. Soc. 122 (2000) 3458.
[3] F. Rogalewicz, Y. Hoppilliard, G. Ohanessian, Int. J. Mass Spectrom. 201 (2000) 307.
[4] F. Rogalewicz, Y. Hoppilliard, G. Ohanessian, Int. J. Mass Spectrom. 206 (2000) 45.
[5] Y. Hoppilliard, F. Rogalewicz, G. Ohanessian, Int. J. Mass Spectrom. 204 (2000) 267.
[6] R.A. Jockusch, A.S. Lemoff, E.R. Williams, J. Am. Chem. Soc. 123 (2001) 12255.
[7] H. Schwarz, D. Schroder, Pure Appl. Chem. 72 (12) (2000) 2319.
[8] P.B. Armentrout, B.L. Kickel, in: B.S. Freiser (Ed.), Understanding Chemical Reactivity, Vol. 15, Kluwer Academic Publisher, Dordrecht, 1996, p. 1.
[9] A. Ricca, C.W. Bauschlicher, M. Rosi, J. Phys. Chem. 98 (1994) 9498.
[10] A. Ricca, C.W. Bauschlicher, J. Phys. Chem. 98 (1994) 12899.
[11] C.W. Bauschlicher, P. Maitre, J. Phys. Chem. 99 (1995) 3444.
[12] J. Allison, R.B. Freas, D.P. Ridge, J. Am. Chem. Soc. 101 (1979) 1332.
[13] P.A.M. van Koppen, M.T. Bowers, C.L. Haynes, P.B. Armentrout, J. Am. Chem. Soc. 120 (1998) 5704.
[14] K.K. Irikura, J.L. Beauchamp, J. Phys. Chem. 95 (1991) 8344.
[15] P. Mourgues, A. Ferhati, T.B. Mc Mahon, G. Ohanessian, Organometallics 16 (1997) 210.
[16] P. Boissel, P. de Parseval, P. Marty, G. Lefevre, J. Chem. Phys. 106 (1997) 4973.
[17] C. Gee, P. Boissel, G. Ohanessian, Chem. Phys. Lett. 298 (1998) 1.
[18] A. Simon, J. Lemaire, P. Boissel, P. Maitre, J. Chem. Phys. 115 (6) (2001) 2510.
[19] M. Doig, U. Wedig, H. Stoll, H. Preuss, J. Chem. Phys. 86 (1987) 866.
[20] N. Sandig, W. Koch, Organometallics 16 (1997) 5244.
[21] T.H. Dunning, P.J. Hay, Methods of Electronic Structure Theory, New York, 1977.
[22] P.J. Stevens, F.J. Devlin, C.F. Chabalowski, M.J. Frisch, J. Phys. Chem. A 98 (1994) 11623.
[23] M.J. Frisch, G.W. Trucks, H.B. Schiegel, G.E. Scuseria, M.A. Robb, J.R. Cheeseman, V.G. Zakrzewski, J.J.A. Montgomery, R.E. Stratmann, J.C. Burant, S. Dapprich, J.M. Millam, A.D. Daniels, K.N. Kudin, M.C. Strain, O. Farkas, J. Tomasi, V. Barone, M. Cossi, R. Cammi, B. Mennucci, C. Pomelli, C. Adamo, S. Clifford, J. Ochterski, G.A. Petersson, P.Y. Ayala, Q. Cui, K. Morokuma, D.K. Malick, A.D. Rabuck, K. Raghavachari, J.B. Foresman, J. Cioslowski, J.V. Ortiz, B.B. Stefanov, G. Liu, A. Liashenko, P. Piskorz, I. Komaromi, R. Gomperts, R.L. Martin, D.J. Fox, T. Keith, M.A. Al-Laham, C.Y. Peng, A. Nanayakkara, C. Gonzalez, M. Challacombe, P.M.W. Gill, B. Johnson, W. Chen, M.W. Wong, J.L. Andres, C. Gonzalez, M. Head-Gordon, E.S. Replogle, J.A. Pople, Gaussian, Inc., Pittsburgh, PA, 1998.
[24] J.B. Foresman, M. Head-Gordon, J.A. Pople, M.J. Frisch, J. Phys. Chem. 96 (1992) 135.
[25] M.E. Casida, C. Jamorski, K.C. Casida, D.R. Salahub, J. Chem. Phys. 108 (1998) 4439.
[26] C.E. Moore, Atomic Energy Levels, Washington, DC, 1971.
[27] G. Ohanessian, W.A. Goddard III, Acc. Chem. Res. 23 (1990) 386.
[28] M.L. Steigerwald, W.A. Goddard III, J. Am. Chem. Soc. 106 (1984) 308.
[29] C. Heinemann, W. Koch, H. Schwarz, Chem. Phys. Lett. 245 (1995) 509.
[30] S. Koseki, M.W. Schmidt, M.S. Gordon, J. Phys. Chem. A 102 (1998) 10430.
[31] L.M. Russon, S.A. Heidecke, M.K. Birke, J. Conceicao, M.D. Morse, P.B. Armentrout, J. Chem. Phys. 100 (1994) 4747.
[32] M. Okumura, L.I. Yeh, Y.T. Lee, J. Chem. Phys. 83 (1985) 3705.
[33] M. Okumura, L.I. Yeh, J.D. Myers, Y.T. Lee, J. Phys. Chem. 94 (1990) 3416.
[34] J. Oomens, G. Meijer, G. von Helden, J. Phys. Chem. A 105 (36) (2001) 8302.
[35] D. van Heijnsbergen, G. von Helden, G. Meijer, P. Maitre, M.A. Duncan, J. Am. Chem. Soc. 124 (2002) 1562.
[36] J.G. Black, E. Yablonovitch, N. Bloembergen, S. Mukanel, Phys. Rev. Lett. 38 (1977) 1131.
[37] LURE, www.lure.u-psud.fr